Rose, A.V., Taylor, R.N. & El Naggar, M. H. (2013). Numerical modelling of perimeter pile groups in clay. Canadian Geotechnical Journal, 50(3), pp. 250-258. doi: 10.1139/cgj-2012-0194

CITY UNIVERSITY LONDON

EST 1894

City Research Online

Original citation: Rose, A.V., Taylor, R.N. & El Naggar, M. H. (2013). Numerical modelling of perimeter pile groups in clay. Canadian Geotechnical Journal, 50(3), pp. 250-258. doi: 10.1139/cgj-2012-0194

Permanent City Research Online URL: http://openaccess.city.ac.uk/6921/

Numerical Modelling of Perimeter Pile Groups in Clay

Rose, A. V. (Dr)

City University London, Geotechnical Engineering Research Group, Northampton Square, London, EC1V 0HB, UK

alexis.rose.1@city.ac.uk

Taylor, R. N. (Prof)

City University London, Geotechnical Engineering Research Group, Northampton Square, London, EC1V 0HB, UK

r.n.taylor@city.ac.uk

El Naggar, M. H. (Dr)

University of Western Ontario, Geotechnical Research Centre, Spencer Engineering Building, 1151 Richmond St, London, Ontario, N6A 5B9, Canada

helnaggar@eng.uwo.ca

Author responsible for correspondence:

Alexis Rose

City University London, Geotechnical Research Group, Northampton Square, London, EC1V 0HB, UK

alexis.rose.1@city.ac.uk

Tel: +44 (0)7989 559385

Abstract

The load distribution among piles in a group varies such that the inner piles often carry a smaller share of the total load compared to the exterior piles, which is a result of increased soil-pile interaction. The main objective of this paper is to establish the relative effectiveness of pile groups with no inner piles (perimeter group), when compared to the more common grid configuration. The numerical investigation utilised the finite element programme ABAQUS and considered a range of variables that affect pile group behaviour including: number of piles, pile spacing, length/diameter ratio and soil strength.

It was demonstrated that a complete grid group was less efficient than a perimeter group, where efficiency is defined as the load capacity of the whole group expressed as a ratio of the number of piles in the group multiplied by the load capacity of a single isolated pile. Efficiencies close to unity were observed for some perimeter groups. Perimeter groups also showed a 'block' type group failure could occur, where piles were placed at a spacing of less than 2.0 d centre-to-centre. This often, but not always, led to a reduction in the efficiency of the pile group.

Key words: Pile groups, mini piles, numerical analysis, efficiency

1   Introduction

It is generally accepted that pile groups in clay have an efficiency of less than one, where efficiency is defined as the load capacity of the whole group expressed as a ratio of the number of piles in the group multiplied by the load capacity of a single isolated pile. In this context, the term 'pile groups' is generally considered to refer to groups in a grid arrangement, e.g. a group of 5x5, consisting of 25 piles. It was unknown if perimeter groups, where all inner piles are removed (Figure 1), would also have an efficiency of less than one. A research project investigated the problem using centrifuge modelling of a range of pile groups, using the facility at City University London (Rose, 2012). The model piles simulated bored piles in firm kaolin clay; they were loaded under monotonic axial loading conditions and tested to failure. Centrifuge testing was complex and extensive and details of the experimental work are beyond the scope of this paper.

A numerical investigation of the problem has been conducted using the finite element (FE) method. The initial analyses agreed with and confirmed the main findings of the centrifuge experiments. Further analyses were undertaken to extend the scope of the experimental research. The variables considered in the analysis include the geometry of the group (shape and length/diameter ratio), the number of piles, the pile spacing and the soil strength. These properties will affect the soil-pile interaction and consequently the behaviour of the group, which will influence the efficiency. Such pile groups may be installed when it is necessary to carry large loads in confined spaces and may provide a more efficient alternative to traditional grid groups, but there is currently little experience of the performance that could be expected.

Numerous studies have investigated the effect of pile spacing on group efficiency, for example: Feld (1943), Whitaker (1957), Saffery and Tate (1961), Terzaghi and Peck (1967), de Mello (1969), Barden and Monckton (1970), Cooke (1974), and O'Neill (1982). Considerable testing was done as part of these previous research efforts to evaluate the influence of pile spacing on group behaviour and efficiency, yet the outcome remained somewhat inconclusive. However, efficiencies generally emerged as less than one, and it is primarily considered that the inner/central piles are the most inefficient.

Randolph (1994) showed that using a few central piles can be more efficient in reducing settlements beneath piled rafts, compared with a grid arrangement of piles. With this as inspiration, an interesting comparison within these experiments has been to test a perimeter group with a single central pile. The term 'target group' is coined for such an arrangement.

2   Numerical Modelling

A range of pile group models were analysed numerically using the FE programme, ABAQUS (Hibbitt et al, 2008). A relatively simple and well understood constitutive soil model has been used in the analysis. The 3D capability along with the range of elements and interface conditions available in this software allows accurate relative comparison between the performances of different group configurations. A summary of the pile groups investigated is shown in Table 1. Each group has a seven character reference, e.g., PC14_1.75, which is explained as follows:

- P   group type (Perimeter, Target, Grid)

- C   group shape (Circle, Square)

- 14   number of piles (ranging from 12 to 25)

- 1.75 centre to centre pile spacing, in pile diameters (ranging from 1.50 to 3.00)

Example configurations of other group types are shown in Figure 2.

2.1 Soil model

Since only the undrained behaviour of the soil was being considered, it was deemed sufficient to use a total stress model for the soil. The behaviour of the soil was simulated by the elastic perfectly plastic stress-strain relationship incorporated within the Tresca failure criterion. This model is implemented into Abaqus as a modification of the Mohr-Coulomb failure criterion and requires the following five parameters: unit weight (γ), cohesion (c), friction angle (ϕ), Young's modulus (E) and Poisson's ratio (ν). The undrained shear strength (s_u) and associated total stress values were used: γ = 1800 kg/m^3, s_u = [various], ϕ = 0, E = 50 MPa and ν = 0.495.

The loading is considered to be applied relatively quickly, therefore pore pressures and the change thereof, have not been accounted for. This soil model is often considered too basic to model real in-situ soils with enough accuracy; but in this instance it was considered acceptable since its primary purpose was to allow a comparison of pile group behaviour, rather than generate absolute values of load capacity.

The soil profile was divided vertically into three 5 m layers over the length of the pile, with a further single layer extending from the pile toe to the base of the model, with a constant s_u value assigned to each layer. This technique of course created an imperfect staggered s_u profile, but a sensitivity analysis was carried out by further dividing the soil into sub-layers and very little difference was observed.

2.2 Soil-pile interface

The soil-pile interface was simulated using the basic concept of Coulomb friction model, which relates the maximum allowable shear stress (friction) across an interface to the contact pressure between the contacting bodies. Hence, the soil and pile surfaces can carry a shear stress up to a certain critical shear stress across their interface before they start sliding relative to one another; this is the state of sticking. The critical shear stress (the point at which sliding starts) is defined as a fraction of the contact pressure between the surfaces. A maximum shear stress, τ_{max}, was set in each of the analyses and was equal to a proportion of the shear strength of the soil. This was chosen to be similar to a typical value of αs_u, where α is the adhesion factor. Setting a value for τ_{max} automatically makes it the controlling factor regardless of the magnitude of the contact pressure.

The piles were divided into three sections, which corresponded with the soil layers to enable appropriate interface values to be applied and therefore the value of τ_{max} varied with depth. The analyses used equivalent prototype pile dimensions of 300 mm diameter, d, and 15 m length, L.

2.3   The mesh

The soil-pile system was simulated using a 3D model that was comprised of solid eight-node hexahedron elements to represent the soil and the piles. The pile cap was modelled with discrete rigid elements and a constraint was established whereby the underside of the pile cap was tied to the tops of the piles. The purpose of the pile cap was to ensure all piles moved simultaneously and by the same amount. The pile cap was positioned sufficiently far above the ground to ensure it did not make contact with the clay surface during loading. Reduced integration elements were chosen because fewer Gaussian integration points are used when solving the numerical integral within the FEA solver, leading to reduced

computation time with little reduction in accuracy. Additionally, displacement-based FE formulations over-estimate the stiffness matrix, so by using fewer integration points a less stiff element is produced, which improves approximation of real-life behaviour. Furthermore, reduced integration elements overcome the 'volumetric locking' effect of excessive stiffness when ν approaches 0.5.

The dimensions of the mesh were such that it extended 2L in height (z-axis) and a distance L in both the x and y axes. A staged mesh refinement was carried out to reach an optimum mesh size. In order to accurately capture the behaviour of piles, the average aspect ratio of elements was kept below 1:4. In high stress concentration regions, the aspect ratio was kept as close to unity as possible. The models were seeded by hand and on the whole the same numbers of seeds were placed in the same locations in each model. There was inevitable variation where the soil surrounded the piles but every attempt was made to ensure that the models had about the same distribution of elements and that the number of elements was kept at approximately 25,000.

In order to reduce the computational time and effort but keep good accuracy, the soil-pile system was simplified to quarter symmetric models. Consequently, symmetry boundary conditions were employed on the vertical 'internal faces'. A fully fixed boundary condition was applied to the base of the model and the vertical 'external faces' were fully fixed in the x and y directions.

2.4   Stress and displacement controls

Geostatic stresses were used to verify that the initial stress field was in equilibrium with the applied loads and boundary conditions at negligible strain. The geostatic stresses assume a

gravitational acceleration of 10 m/s^2 and were applied in the first step, prior to pile installation. The affect of this step is to generate increasing stress with depth with only minute strains and in doing so replicate prototype stress conditions. The horizontal stresses were directly proportional to the vertical stresses in all models, and for these analyses K = σ_h/σ_v = 1. The loading was displacement controlled, which was applied over the surface of the pile cap, with zero allowance of pile cap rotation.

3   Numerical Analysis

3.1   Verification

As part of the verification process, the response of a single pile installed in a range of soil profiles were calculated by hand to ensure the numerical analyses were behaving in an expected manner and to allow calculations of group efficiency. In addition, the numerical results were compared with the already existing experimental results (Rose, 2012). At equivalent prototype scale, the average capacity of a single pile obtained from the centrifuge tests equated to 533 kN. The capacity calculation using the method described by Skempton (1959) gives a single pile capacity of 487 kN, when using the soil properties akin to the soil used for the centrifuge tests. The standard soil profile (soil profile A, sp$_A$) selected for the numerical models was chosen to reflect the s$_u$ profile of the centrifuge tests. All soil profiles used in the numerical analyses are shown in Figure 3. The single pile peak capacity calculated by the numerical model for sp$_A$ was 538 kN at a settlement corresponding to 0.30 d, which is a difference of only 1 % compared with the centrifuge result and about 10 % compared with the calculation. This degree of settlement is greater than that used in design and it is important to note that pile group efficiency within these analyses are calculated using single pile capacities at corresponding settlements. For example, when considering the efficiency

of a pile group at 0.05 d settlement, the capacity of the single pile at a settlement of 0.05 d will be used in that calculation. This is discussed further in the following section.

3.2   Single pile

The load vs settlement curve for a single pile in soil profile sp_A is shown in Figure 4, where settlement is expressed as a fraction of the pile diameter. It can be observed that the pile experienced plunging failure, and the peak load can be considered as the ultimate capacity of the pile. The group loads at three stages of settlement (0.02, 0.05 and 0.10 d) were compared with the single pile also at those stages of settlement. No comparisons were made beyond a settlement of 0.10 d, since the majority of load will have been mobilised by a settlement of 10 % pile diameter, as described by previous Authors (e.g. Burland and Cooke, 1974; Fleming et al, 2009) and also found within this research.

3.3   Perimeter groups

Five perimeter groups were analysed to investigate groups thought to be on the boundary of transition between the two types of failure mechanism (individual and block). As a result, only a relatively narrow range of groups were tested.

A summary of the data is shown in Table 2. The values displayed are the calculated efficiencies as compared to a single pile at the particular stages of settlement stated. As can be noted from Table 2, all groups with piles spaced at 1.75 d (but with different numbers of piles) show very similar results. The group with pile spacing at 1.5 d displayed lower efficiencies. For example, the efficiency at 0.1 d settlement (interpreted failure load) varied from 0.79 for pile spacing of 1.5 d, to 0.92 for pile spacing of 1.75 d. The efficiency at 0.02 d settlement (serviceability or performance condition) was similar for all groups.

The results of a selection of groups are shown in Figure 5. The two larger groups, PS20_1.75 and PC14_1.75 had the same pile spacing (1.75 d) and showed a similar response profile, whereas group PC12_1.50, with pile spacing of 1.5 d, displayed a more prominent peak efficiency that subsequently reduced. This is possibly caused by the initial engagement of the central core of soil and maximum soil-soil and soil-pile shearing as a block failure mechanism developed. Once the block mechanism has fully mobilised and the central soil is moving downwards by the same (or similar) amount as the piles, the failure interface becomes predominantly soil-pile for this group with more closely spaced piles.

3.4   Target groups

Five target groups were analysed and the efficiencies are summarised in Table 3. The results of a selection of groups are shown in Figure 6. The group with the highest efficiency is TC16_2.00 and interestingly, this circular group shows a slightly higher efficiency than the equivalent square group. The group with the lowest efficiency is TC14_1.75; as with the perimeter groups, this is the group with the closest spacing and the fewest number of piles.

One group was tested as both a perimeter and target group (as highlighted in Tables 2 and 3). The addition of the central pile seems to make little difference to the efficiency, but it did increase the settlement of the central soil. Figure 7 shows PS16_2.00 and TS16_2.00, which illustrates the effect of the central pile in dragging down the central soil. The central soil of group TS16_2.00 settled by approximately 50 mm. One disadvantage of the simplified numerical model that became apparent was its inability to accurately simulate the formation of a shear surface, despite sometimes large displacements occurring.

3.5   Grid groups

Four grid groups were analysed; a summary of the data is given in Table 4 and the results are shown in Figure 8 (apart from GS25_3.00, which did not converge). The results show that at a settlement of 0.10 d, GS16_2.00 had a similar efficiency to GS25_3.00 but had a higher efficiency than the group of 25 piles that is also spaced at 2.0 d. This is perhaps not surprising considering that in the group of 25 piles, nine were inner piles (i.e. 36 % are inner piles). For the group of 16 piles, four are inner piles (25 %), thus the group of 25 piles is less efficient. Whitaker (1957) and Barden and Monckton (1970) also showed that a group of 25 piles at 2.0 d centres achieved an efficiency of about 0.8.

The group spaced at 3.0 d suffers less from the effect of neighbouring piles, and the group spaced at 1.5 d suffers considerably more, with an efficiency of just 0.54 at a settlement of 0.10 d.

3.6   Varying soil strength

The soil profiles B (sp_B), C (sp_C) and C2 (sp_{C2}) were tested for comparison against the standard soil profile, sp_A. In general terms, sp_B is double the strength of sp_A and sp_C is half the strength of sp_A (refer back to Figure 3). Soil profile sp_{C2} has the same strength as sp_C, but has soil stiffness reduced by half. A summary of groups tested is shown in Table 1.

Efficiency comparisons were carried out at the same stages of settlement and the results are presented in Table 5. Also shown is the degree of settlement of the central soil, expressed as the ratio settlement of central soil (δ_s) : settlement of pile (δ_p). This is an indicator of failure mechanism: $\delta_s/\delta_p = 0$ indicates individual pile failure; $\delta_s/\delta_p \rightarrow 1$ indicates block failure. Four groups were tested in the stronger soil. The two target groups and one perimeter group each show an initial decrease in efficiency at the lowest settlement stage within the stronger

soil, compared to the standard soil. At a settlement of 0.05 d there was very little difference between soil profiles. Finally, at 0.10 d settlement, the three groups showed a slightly higher efficiency in the stronger soil.

For the grid group, the results are quite different. As the settlement progresses the efficiency becomes increasingly higher in the stronger soil, compared with the standard soil. It can be noted from the ratio δ_s/δ_p that all groups behaved individually in the stronger soil, except for the grid groups. Only group GS25_2.00 was tested with soil profile sp_C and sp_{C2} and the results showed the efficiency was always lower in the softer soil. At a settlement of 0.10 d, the efficiency is only 0.54 in sp_C, compared with 0.71 in sp_A and 0.98 in sp_B. The softer soil with lower stiffness showed a lower efficiency than sp_C, but this was only noticeable at the lowest stage of settlement. At other stages of settlement the results of sp_C and sp_{C2} were comparable.

The observed behaviour suggests that a stronger soil leads to higher group efficiencies and this effect is most pronounced in grid groups.

3.7   Varying l/d ratio

To explore the effect of pile slenderness ratio, l/d, two cases were considered in the analysis, l/d = 50 (standard) and 100. The pile length (15 m) was kept constant, but the diameter was reduced from 300 mm to 150 mm. The results are summarised in Table 6.

The efficiency of the slender piles are compared to the standard groups (l/d = 50). The slender pile groups experienced a reduction in central soil settlement. At 0.10 d settlement, the slender piles saw in an increase in the group efficiency for GS25_2.00 and PS20_1.75, but a reduction for TS16_2.00. This difference is perhaps caused by the fact that the slender

piles lead to only a reduction in central soil settlement for GS25_2.00 and PS20_1.75, but cause a complete cessation of central soil movement in TS16_2.00, which means there is no soil-soil shear, and hence a reduction in capacity.

4   Soil stresses and movements

In order to assess the soil stresses and movements, a single pile group has been considered in two different soil profiles. Group PS20_1.75 has been analysed both in soil profile A (sp_A) and soil profile B (sp_B). This group was chosen because it was a perimeter group that experienced different failure mechanisms in differing soil profiles. Group PS20_1.75 fails as a block in sp_A and fails as individual piles in sp_B as demonstrated in the following discussion.

4.1   Soil Response

To further understand the performance of perimeter pile groups, the following components were evaluated: the vertical stress, the horizontal stress, the vertical displacement and the horizontal displacement. The horizontal variables were analysed along three vertical paths on the y-axis; one path is inside the group and two are outside, as depicted by the dashed lines in Figure 9 (which shows the mesh y-z plane and an approximate location of the nearest pile). The vertical variables were recorded along the following three horizontal paths: 2 m (near pile top), 8 m (near pile middle) and 16 m (beneath pile toe), also depicted in Figure 9. The data were taken from the following stages of pile settlement: 0.01, 0.02, 0.05 and 0.10 d.

4.1.1 Soil stresses

To track the changes in vertical stress, the magnitude of stress at the defined stages of settlement has been plotted as a ratio of the initial geostatic stress, as shown in Figures 10 and 11. The origin is placed at the centre of the group, the x-axis is outward to the model boundary and the right-hand y-axis is the depth of the path through the model. The left-hand y-axes show the calculated stress divided by the initial stress, with three individual axes for each depth considered within the model. As a consequence, values that plot higher than 1 on the y-axis represent an increase in stress (relative to the initial in-situ stress) as displacement proceeds, and values that plot lower than 1 represent a decrease in stress.

The vertical stresses for the different soil profiles are shown in Figures 10 and 11 for sp_A and sp_B, respectively. At z = 2 m, there is an initial small increase and then a reduction in stress in both sp_A and sp_B, although the reduction in sp_A is more pronounced close to the pile. At z = 8 m, there is an increase in stress in sp_A and no changes in stress in sp_B. Finally, at z = 16 m, there is an increase in stress in both soil profiles, but the increase is distributed more evenly in sp_A, whereas the increase is more highly concentrated beneath the pile toe in sp_B. This indicates that the core soil tends to deform vertically in both soil profiles, but this is more evenly distributed over the pile length in sp_B, whereas it appears to be more concentrated over the top half of the pile in sp_A. This may be what influences the formation of a block failure mechanism.

Similar illustrations of results for the horizontal stresses are shown in Figures 12 and 13. The y-axis represents the depth along the model; the top x-axis is the distance from the group centre, with paths at 0.5 m 1.5 m and 2.5 m; the bottom x-axis shows the recorded stress as a ratio of the initial stress, with each path having a separate axis. Stresses within the top 5 m are rather different between soil profiles and the stress in sp_B becomes increasingly higher.

The stresses in sp_A begin increasing, but then show a reduction at a settlement of 0.10 d. However, it should be noted that the results are displayed as a ratio of the initial stress, which is very low near the surface and so a stress ratio several times higher is not necessarily a high stress in absolute terms. As may be expected, just below the horizon of the pile toe, horizontal stresses have increased. However, for sp_B, there is a region just above the toe of the piles where the stresses appear to have decreased, particularly just on the outside of the group. The stress profiles show slight anomalies at depths of 5 m and 10 m where there is a step change in the undrained strength. These are localised and are not considered to affect the overall behaviour.

4.1.2 Soil movements

The vertical soil movements for sp_A are shown in Figure 14. The path profiles are the same as those for the calculated vertical stresses, at depths of 2 m, 8 m and 16 m from the soil surface. The vertical settlement of the core soil is about 30 mm, clearly demonstrating that the group has experienced block failure. In sp_B, the vertical settlement was found to be considerably less, as shown in Figure 15. There was only a few millimetres difference between the settlement on the inside and outside of the group, and the group experienced individual pile failure. Beneath the piles, the vertical settlement is much less for sp_A, just over 10 mm.

In general, the soil moved horizontally outwards away from the pile group with larger movements in sp_A than in sp_B. However, for sp_A, the soil moved inwards at the pile heads and some small outward movement above the pile base. On the other hand, there is almost no movement at the pile heads for sp_B and some movement below the pile base. The base movements are very small and have not been reproduced graphically.

It is clear that groups which fail via the block mechanism suffer significant settlement of the soil core. The constant volume deformation of undrained soil means the only logical explanation is that the core soil has been displaced downwards, causing the soil outside the group to move upwards resulting in an increase in the overall soil elevation outside the group. A diagram of these hypothesised movements and stresses associated with block failure are shown in Figure 16.

5   Design considerations

Fleming et al (2009) discussed the failure of a pile group and stated that independent calculations should be made of both the block capacity and the individual pile capacities, to ensure that there is an adequate factor of safety against both modes of failure. The axial capacity of a group failing as a block may be calculated the same way as for a single pile but using the group perimeter, P, and area, A, for the whole block when calculating its shaft and base contributions. It should be noted that the settlement needed to mobilise the base capacity of the block will usually be very large (i.e. 5 to 10 % the width of the group). Therefore, if the benefits of any base capacity can be exploited in perimeter groups then it is probable that these settlements will also be large. The increased settlement necessary to fully mobilise the base capacity may limit the application of perimeter groups, except for less sensitive structures. However, it should be noted that there were no signs of significant base capacity mobilisation from the numerical modelling. This was also the case in the centrifuge experiments (Rose, 2012).

In order to facilitate the implementation of perimeter groups in foundation design, it would be preferable to define an efficiency value for each group. However, the range of variables involved and the associated complexity of assigning a value to each group have been

illustrated. In addition, designs will have differences regarding settlement tolerances and design parameters, so specific guidance is not appropriate at this stage.

For general guidance and preliminary design, Figure 17 presents the group efficiency vs settlement for a range of groups. If a simple single pile design is completed, then once this capacity has been multiplied by the number of piles in the group, these curves can be used to approximate the efficiency of the group and consequently its capacity. Of course, this should be used along with the appropriate factor of safety.

6 Summary of main findings

A range of perimeter, target and grid groups have been investigated numerically, along with single piles tests, in order to evaluate group efficiencies. Perimeter groups containing 14 to 20 piles and spaced at 1.75 d experienced block failure and achieved efficiencies of about 0.9. A group of 12 piles spaced at 1.5 d initially had a similar efficiency, but this reduced to 0.8 by a settlement of 0.10 d. Results of an equivalent circular and square target group showed the circular group had a slightly higher efficiency, perhaps caused by the larger volume of soil in the central core, which is engaged in the shearing mechanism. Grid group tests demonstrated similar results to those previously found by other Authors. The results also showed a significant difference in efficiency between a group of 25 piles spaced at 3.0 d (0.8) and spaced at 1.5 d (0.5).

It was found that a stronger soil led to a slightly higher efficiency in perimeter and target groups and a substantially higher efficiency in grid groups, when compared with the standard soil. The stronger soil often led to groups failing as individual piles, where the same group had undergone block failure in the standard soil. Piles with a higher l/d ratio caused a

reduction in core soil settlement and, in some cases, an associated increase in efficiency. However, when core soil settlement was not developed at all, this led to a decrease in efficiency. The changes in failure mechanism and efficiency that have been discussed are as a result of changes in soil-pile interaction, which is a direct consequence of group geometry and soil strength. The variation of interaction causes subtle changes in vertical and horizontal stresses within the soil, which inevitably affects the movements of the soil. Engagement of the central soil is considered an important factor and requires optimal group geometry, where maximum soil-soil shear can occur.

Acknowledgements

References

Barden, L. and Monckton, M. F. (1970). Tests on model pile groups in soft and stiff clay. Géotechnique, Vol. 20, No. 1, pp 94-96.

Burland, J. B. and Cooke, R. W. (1974). The design of bored piles in stiff clays. Ground Engng, Vol. 7, No. 4, pp 28-35.

Cooke, R. W. (1974). Piled foundations: A survey of research at the building research station. Building Research Establishment.

De Mello, V. F. B. (1969). Foundations of buildings on clay. State of the art report. Proc. 7th Int. Conf. Soil Mech. & Found. Engng. Mexico City, pp 49-136.

Feld, J. (1943). Discussion on friction pile foundations. Trans. Amer. Soc. Civ. Engrs. 108, pp 143-144.

Fleming, W. G. K., Weltman, A. J., Randolph, M. F. and Elson, W. K. (2009). 3rd Ed. Piling Engineering. Taylor and Francis, Abingdon.

Hibbitt, D., Karlsson, B. and Sorensen, P. (2008). ABAQUS 6.8: A computer software for finite element analysis. Hibbitt, Karlsson and Sorensen Inc., Rhode Island, USA.

O'Neill, M. W., Hawkins, R. A. and Mahar, L. J. (1982). Load transfer mechanisms in piles and pile groups. J. Geotech. Eng. ASCE, Vol. 108, No. 12, pp 1605-1623.

Randolph, M. F. (1994). Design methods for pile groups and piled rafts. Proc. 13th Int. Conf. Soil Mech. and Found. Engng, New Delhi. Vol. 5, pp 61-82.

Rose, A. V. (2012). Behaviour and efficiency of perimeter pile groups. PhD Thesis, School of Engineering and Mathematical Sciences, City University London.

Saffery, M. and Tate, A. P. K. (1961). Model tests on pile groups in clay soil. Proc. 5th Int. Conf. Soil Mech, Paris, Vol. 2.

Skempton, A. W. (1959). Cast in-situ bored piles in London Clay, Géotechnique, No. 9, pp 153 – 173.

Terzaghi, K. and Peck, R. B. (1967). 3rd Ed. Soil Mechanics in Engineering Practice. John Wiley & Sons, New York.

Whitaker, T. (1957). Experiments with model piles in groups. Géotechnique, Vol. 7, No. 4, pp 147-167.

Figure list and captions

Table 1 Summary of groups tested

Group	standard (spA)	l/d = 100 (spA_100)	higher soil strength (spB)	lower soil strength (spC)	low strength & stiffness (spC2)
Single	✓	✓	✓	✓	✓
PC14_1.75	✓				
PC16_1.75	✓				
PC20_1.75	✓				
PC12_1.50	✓				
PS20_1.75	✓	✓	✓		
TC14_1.75	✓		✓		
TC14_2.00	✓				
TC16_2.00	✓				
TS16_2.00	✓	✓	✓		
TS20_2.00	✓				
GS25_1.50	✓				
GS25_2.00	✓	✓	✓	✓	✓
GS25_3.00	✓				
GS16_2.00	✓				

Table 2 Perimeter group data

group	efficiency		
	0.02 d	0.05 d	0.10 d
[†] PC14_1.75 (spA)	0.89	0.95	0.92
PC16_1.75 (spA)	0.89	0.94	0.91
PC20_1.75 (spA)	0.89	0.94	0.92
PC12_1.50 (spA)	0.89	0.87	0.79
PS20_1.75 (spA)	0.88	0.94	0.92

[†] also tested as a target group

Table 3 Target group data

group	efficiency		
	0.02 d	0.05 d	0.10 d
[†] TC14_1.75 (spA)	0.89	0.94	0.90
TC14_2.00 (spA)	0.90	0.96	0.95
TC16_2.00 (spA)	0.90	0.98	0.99
TS16_2.00 (spA)	0.89	0.98	0.96
TS20_2.00 (spA)	0.87	0.94	0.92

[†] also tested as a perimeter group

Table 4   Grid group data

group	efficiency		
	0.02 d	0.05 d	0.10 d
GS25_1.50 (sp_A)	0.65	0.58	0.54
GS25_2.00 (sp_A)	0.76	0.79	0.71
GS25_3.00 (sp_A)	0.81	0.85	0.83
GS16_2.00 (sp_A)	0.86	0.92	0.82

Table 5   Varying soil strength

Group	efficiency			$\delta_s{:}\delta_p$
	0.02 d	0.05 d	0.10 d	
GS25_2.00 (sp_A)	0.76	0.79	0.71	1
GS25_2.00 (sp_B)	0.77	0.91	0.98	0.8
PS20_1.75 (sp_A)	0.88	0.94	0.92	0.7
PS20_1.75 (sp_B)	0.83	0.93	0.95	0
TC14_1.75 (sp_A)	0.89	0.94	0.90	0.8
TC14_1.75 (sp_B)	0.85	0.95	0.97	0
TS16_2.00 (sp_A)	0.89	0.98	0.96	0.5
TS16_2.00 (sp_B)	0.85	0.97	1.00	0
GS25_2.00 (sp_C)	0.53	0.53	0.54	1
GS25_2.00 (sp_{C2})	0.36	0.50	0.52	1

Table 6   Varying l/d ratio

Group	efficiency			$\delta_s{:}\delta_p$
	0.02 d	0.05 d	0.10 d	
PS20_1.75 (sp_A)	0.88	0.94	0.92	0.7
PS20_1.75 (l/d=100_sp_A)	0.86	0.95	0.97	0.4
TS16_2.00 (sp_A)	0.89	0.98	0.96	0.5
TS16_2.00 (l/d=100_sp_A)	0.82	0.88	0.90	0
GS25_2.00 (sp_A)	0.76	0.79	0.71	1
GS25_2.00 (l/d=100_sp_A)	0.76	0.86	0.80	0.8

pile not to scale

standard dimensions
= 300 mm x 15 m
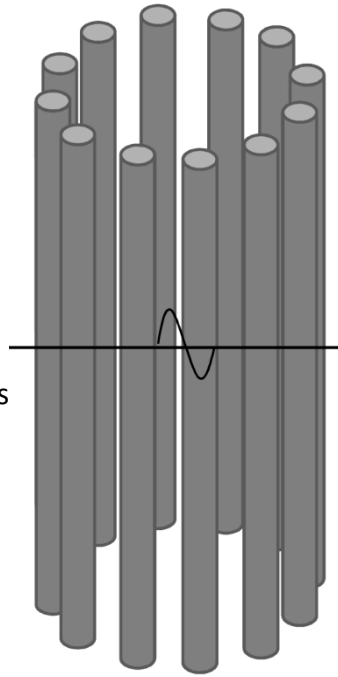
pile not to scale
standard dimensions
= 300 mm x 15 m
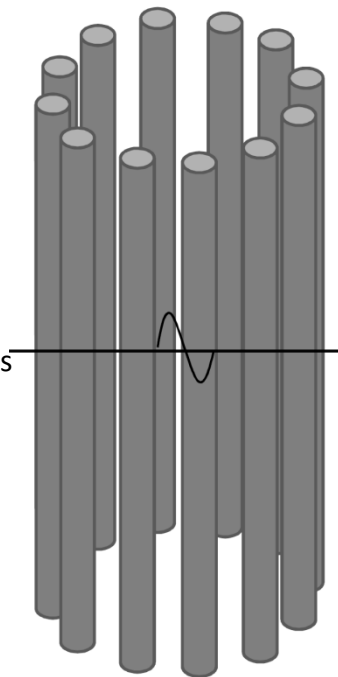
Figure 1   3D view of a circular perimeter pile group, group reference: PC12_2.00

PC12_2.00   PC12_1.50   TC12_2.00

PS12_2.00   TS12_2.00   GS16_2.00
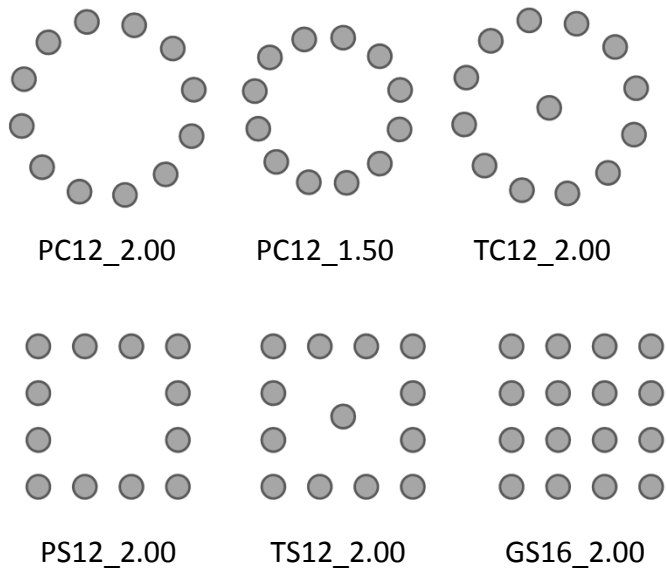
Figure 2   Plan view of group PC12_2.00 and examples of other group types
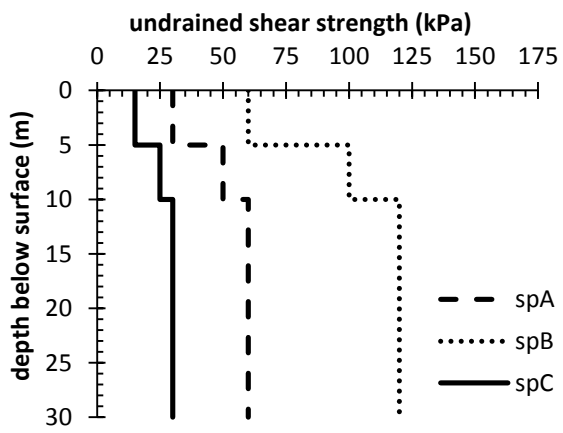
Figure 3   Soil profiles sp_A, sp_B and sp_C
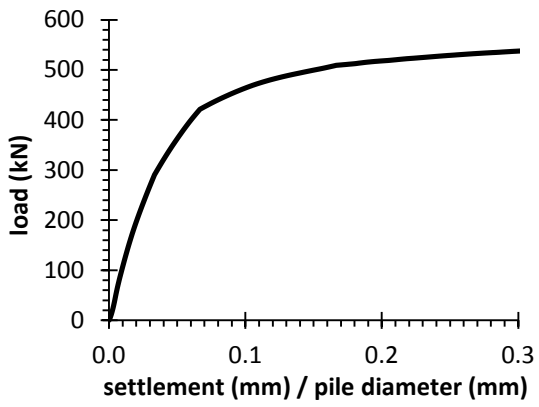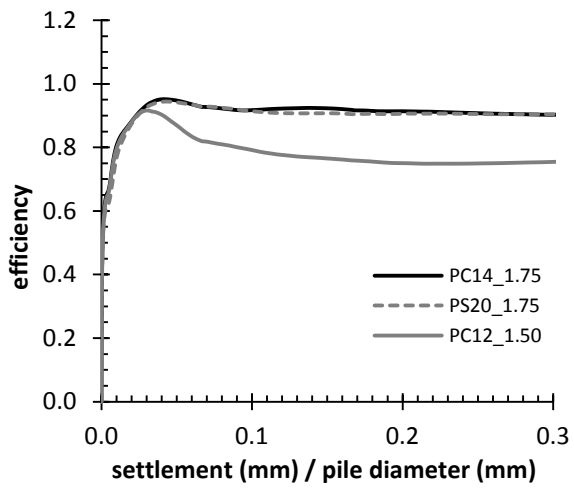
Figure 4   Load vs settlement: single pile (sp$_A$)

Figure 5   Perimeter group results (sp$_A$)
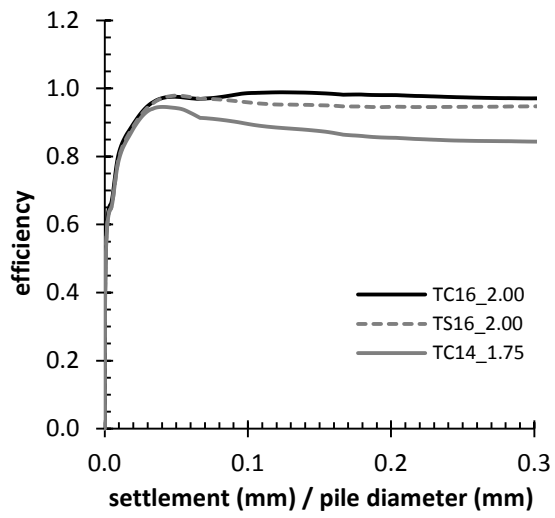
Figure 6   Target group results (sp$_A$)
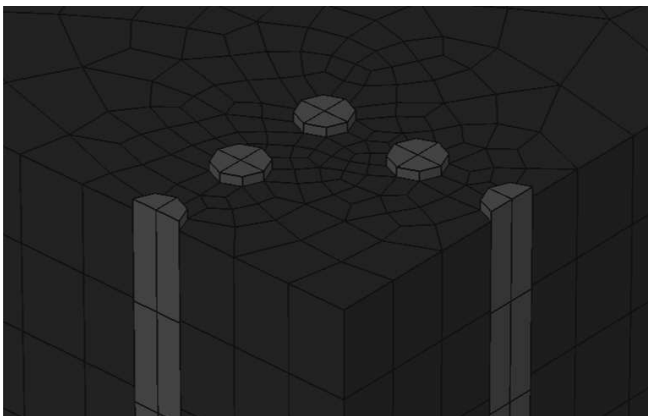
(a)
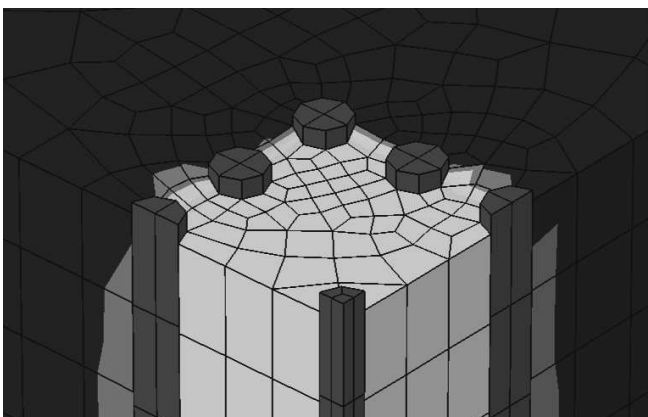
(b)

Figure 7   Numerical output showing central soil settlement of (a) PS16_2.00, and (b) TS16_2.00
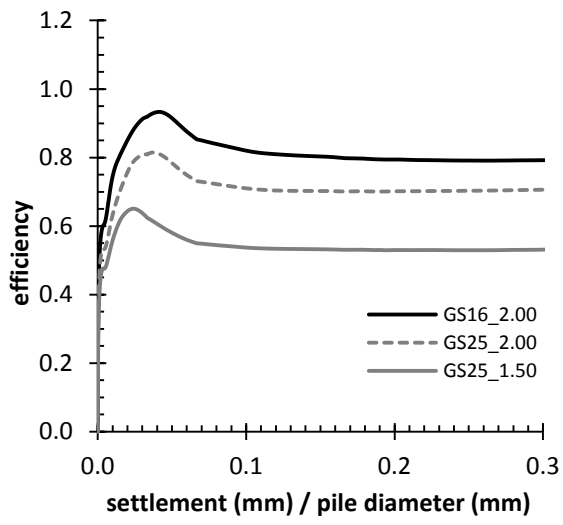
Figure 8   Grid group results (sp_A)
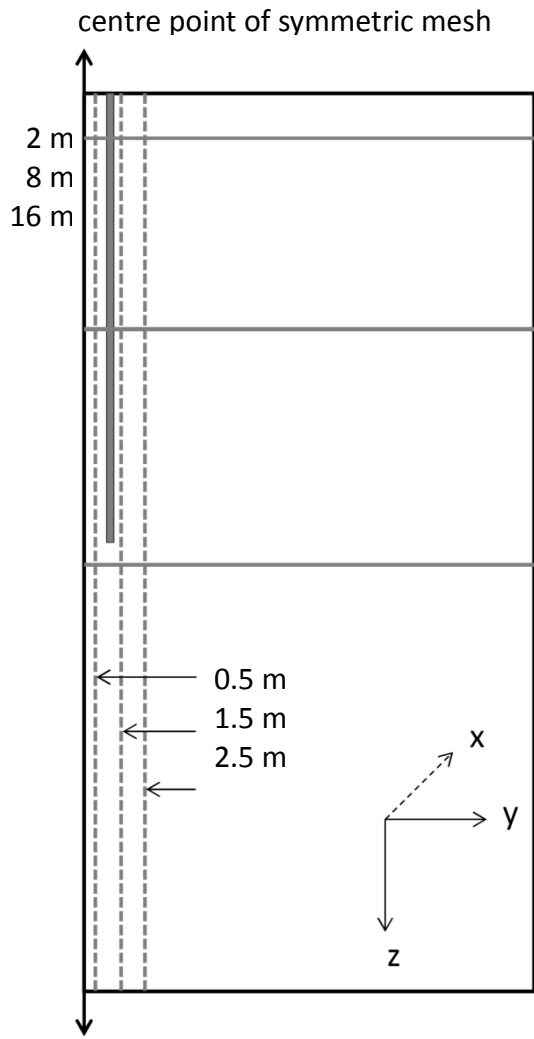
Figure 9   Analysis paths

Figure 11   Vertical stress change (PS20_1.75, sp_B)
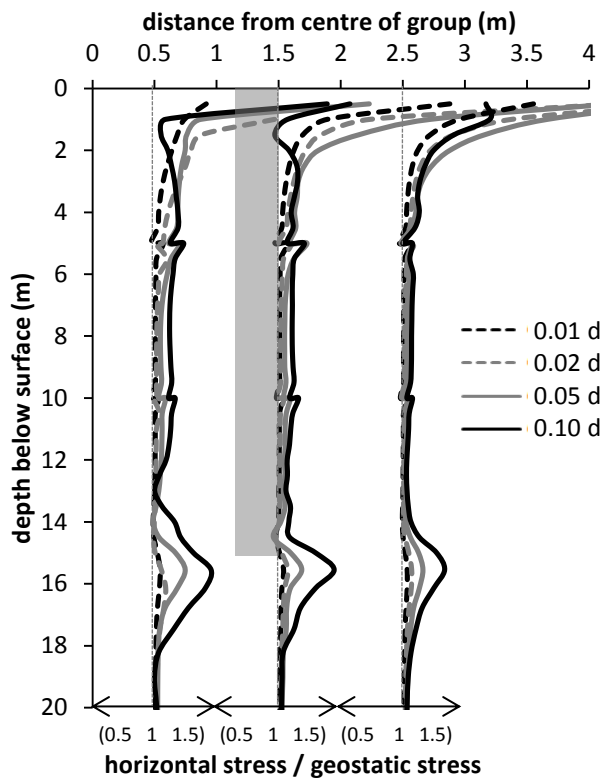

Figure 10   Vertical stress change (PS20_1.75, sp_A)
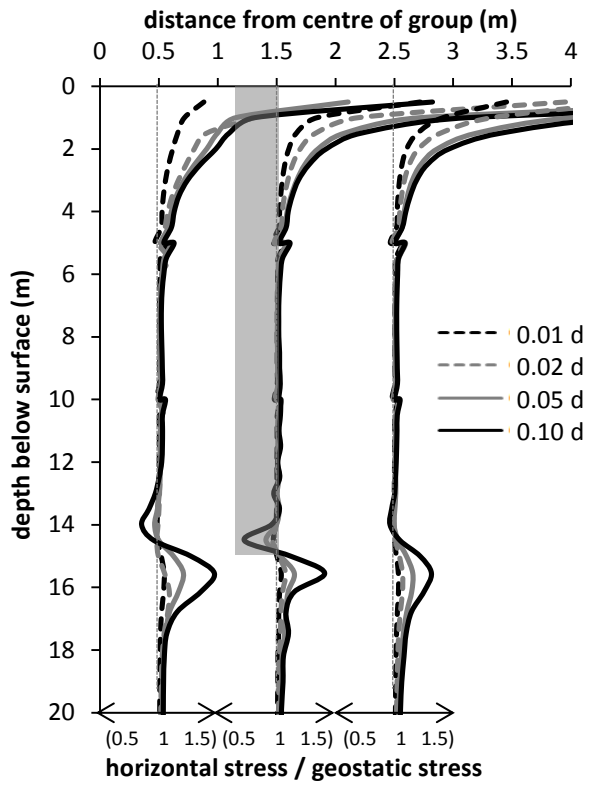
Figure 12   Horizontal stress change (PS20_1.75, sp$_A$)

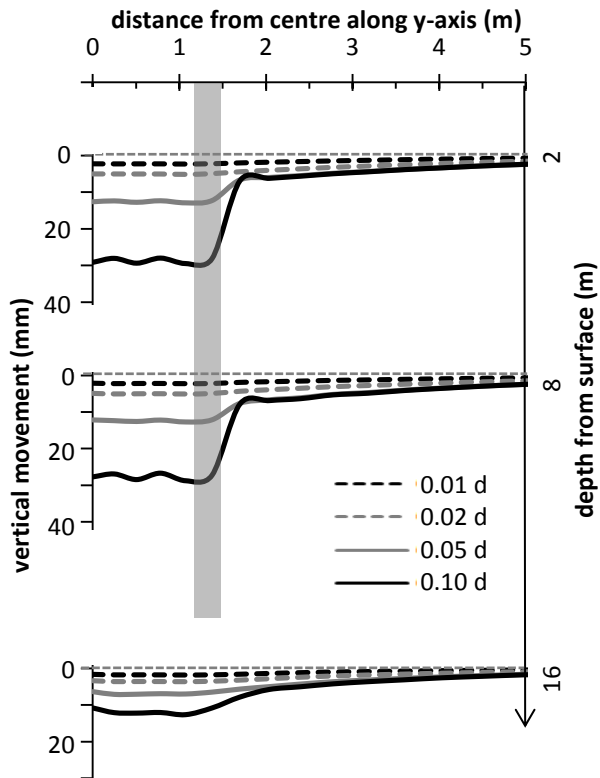Figure 13   Horizontal stress change (PS20_1.75, sp_B)

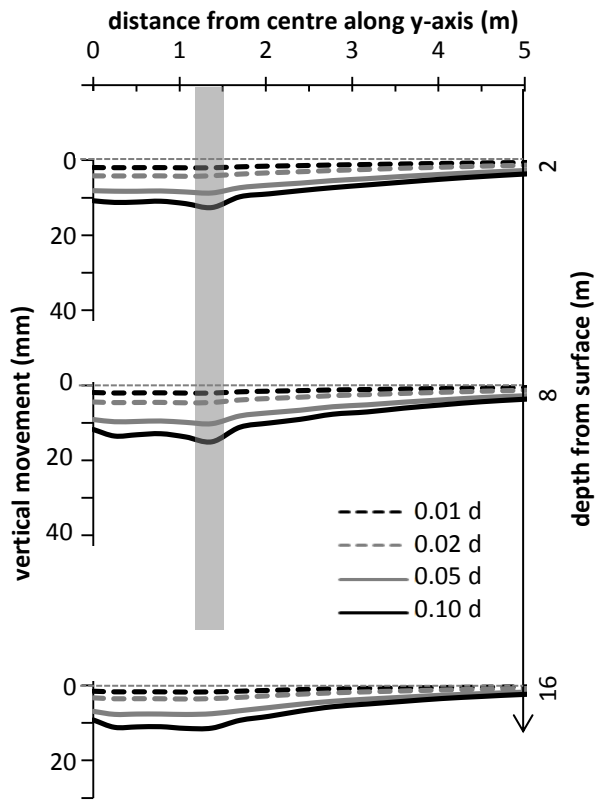Figure 14   Vertical movements (PS20_1.75, sp_A)

Figure 15   Vertical movements (PS20_1.75, sp$_B$)

change from initial

soil level pre-loading
- - - - - - - -

low   high   magnitude of
$\longrightarrow$ $\Longrightarrow$ stress

soil level post-loading
- - - - - - - -

$\rightarrow$ $\longrightarrow$ magnitude of
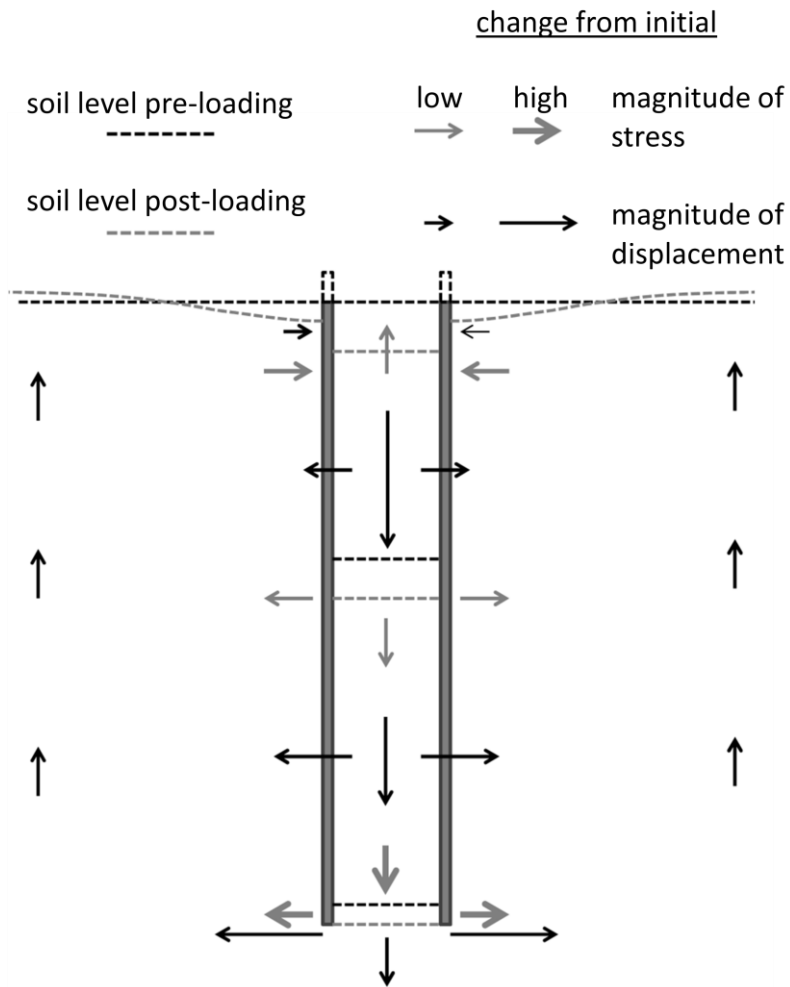displacement

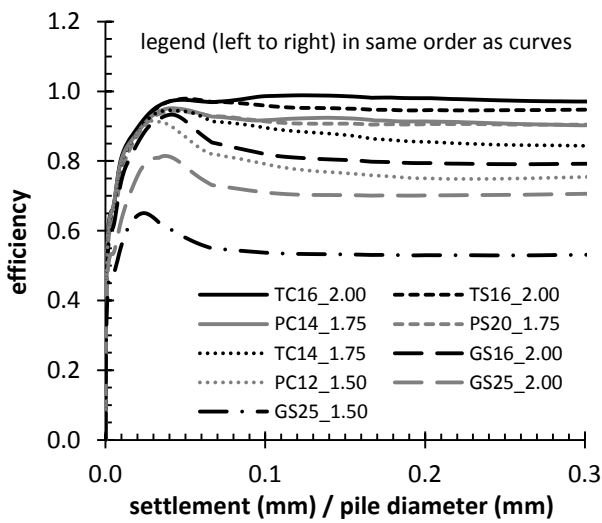Figure 16   Predicted stresses and movements associated with block failure

Figure 17   Design graph: efficiency vs settlement